ORGANIZATION FOR NUCLEAR RESEARCH

An Experimental Test of Exchange Degeneracy in the Hypercharge Exchange Reactions $\pi^+p \to K^+\Sigma^+$ and $K^-p \to \pi^-\Sigma^+$

A. Berglund[1], T. Buran[2], P.J. Carlson[1], C.J.S. Damerell[3], I. Endo[4], A.R. Gillman[3], V. Gracco[5], R.J. Homer[6], M.J. Hotchkiss[3], A. Lundby[2], M. Macri[5], B.N. Ratcliff[7], A. Santroni[5], T. Tso[8], F. Wickens[3], J.A. Wilson[6]

Geneva - December 12th 1977
(Submitted to Physics Letters)

---

1 University of Stockholm, Sweden. Present address: CERN
2 CERN, Geneva, Switzerland
3 Rutherford Laboratory, Chilton, Didcot, Oxon, England
4 CERN. Present address: Phys. Dept., University of Hiroshima, Japan
5 Instituto di Fisica dell´Universita, INFN, Sezione di Genova, Italy
6 Physics Dept., University of Birmingham, England
7 Rutherford Laboratory. Present address: SLAC
8 Rutherford Laboratory. Present address: Brookhaven Nat. Lab.

Abstract.

For the first time, the line reversed reactions $\pi^+p \to K^+\Sigma^+$ and $K^-p \to \pi^-\Sigma^+$ have been studied in the same apparatus. We present the differential cross-sections and polarizations over a large t range and at two momenta, 7.0 and 10.1 GeV/c. The differential cross-sections as a function of t are shown for the first time to cross over. Going from the lower to the higher momentum, the differences in cross-section between the two reactions diminish at low $|t|$ by about a factor 2. We find large polarizations of opposite sign for the two reactions. The momentum dependence, presented in the form of $\alpha_{eff}(t)$ for the t range 0 to -2 $(GeV/c)^2$, is compared with the expectations from the K*-K** trajectory.

In this paper, we present the final results from an experiment whose initial objective, already published[1], was the comparison of the differential cross-sections for the reactions

$$\pi^+ p \to K^+ \Sigma^+ \qquad (1)$$

$$K^- p \to \pi^- \Sigma^+ \qquad (2)$$

at 10.1 GeV/c incident momentum, and over the range in four-momentum-transfer-squared $t_{min} > t > -0.3$ (GeV/c)²†. The experiment was subsequently extended to cover a much larger range in t (out to -2.5 (GeV/c)²) and to include a measurement of the Σ polarization. Finally the experiment was repeated at a lower momentum (7.0 GeV/c) to determine the s-dependence of the cross-sections and polarizations. The results of all phases of the experiment are reported here.

Previous measurements[2] of reactions (1) and (2) at momenta above the s-channel resonance region have not permitted detailed comparisons, because of the significant differences in normalization between different experiments. In addition, there were no high statistics measurements of reaction (2) above 5 GeV/c.

In the simplest theoretical picture, the two processes should be dominated at high energy and small |t| by a pair of exchange Reggeons (corresponding to the K*(890) and K**(1420)). If these trajectories are exchange degenerate and have equal residues, we would expect equal cross-sections and zero polarizations (strong exchange degeneracy). On the other hand, if the K* and K** trajectories are degenerate but the residues are not equal, we expect equal cross-sections, and polarizations which are equal but opposite in sign for the two reactions (weak exchange

---

†t_{min} is the four-momentum-transfer-squared for scattering at 0°. We also use the variable $t' = t - t_{min}$.

For reaction (1),

$t_{min} = -0.0100$ (GeV/c)² at 7.0 GeV/c and -0.0067 (GeV/c)² at 10.1 GeV/c

For reaction (2),

$t_{min} = +0.0087$ (GeV/c)² at 7.0 GeV/c and $+0.0061$ (GeV/c)² at 10.1 GeV/c

degeneracy). These predictions[3] provided the motivation for the present experiment. It had been known for some time that the polarizations were non-zero, but improved polarization measurements (in particular for reaction (2)) and an accurate measurement of the differential cross-sections remained of great interest. In this paper we report the results of the comparison between these predictions and the new data.

The experiment was done in three phases. In the first phase[1], the 10.1 GeV/c beam passed through the active areas of the forward spark chambers. Thus we could measure the differential cross-sections down to 0^0, with small systematic error in normalization but with no polarization measurement. Owing to the limited tolerable beam intensity, this phase was restricted to the t region where the cross-section was large.

Subsequently (Fig. 1), we extended the t range and measured the polarization by adding a recoil arm to the spectrometer and by running the beam outside the active areas of the forward spark chambers. The recoil arm consisted of six gaps of spark chambers with capacitive read-out, followed by a scintillation counter hodoscope with two planes of counters separated by 1 cm of aluminium. A counter box was added round the hydrogen target to veto events with extra charged particles. These veto counters were shielded from the target by metal plates of sufficient thickness to stop δ electrons produced in association with good events. This phase of the experiment was run with a high beam intensity ($\sim 3 \cdot 10^6$ per second). The polarization was determined by measuring the asymmetry in the distribution of the decay protons (from $\Sigma^+ \to p\pi^0$) with respect to the normal to the production plane.

In the third phase of the experiment, the 2-arm set-up was used with a 7.0 GeV/c beam. In order to extend the measurement down to small $|t|$ where no recoil particle was seen, and to increase the geometrical acceptance for intermediate t values, events satisfying only the forward arm trigger logic were also accepted for some of the data taking. As the beam was outside the active areas of the spark chambers, we could not measure down to 0^0, but had a cut-off at $t'=-0.05$ $(GeV/c)^2$.

The experiment took data for 42 days and produced 8 million triggers. The fraction of triggers which were good events of type (1) or (2) varied between 1.2% for 2-arm K^- at 7.0 GeV/c and 0.21% for 1-arm K^- at 10.1 GeV/c, where the dominant source of triggers was $K_{\pi 2}$ decay. In total, we obtained 12500 events of reaction (1) and 7900 events of reaction (2).

The trigger conditions, missing mass resolution and elimination of background have been discussed in detail[1] for the 1-arm data. Adding the requirement of a measured recoil tightened the trigger so that the background trigger rate was reduced. The use of higher beam intensity, however, resulted in a small accidental contribution, even in the fully analysed data. Thus we have backgrounds under the Σ peak due to such reactions as $\pi^+p \to \pi^+\Delta^+$ and $K^+p \to K^+\Delta^+$. Apart from the well-determined tail of the $\Sigma(1385)$, we estimate the backgound within the Σ mass cut to be at worst $2\pm1\%$ (for the low $|t|$ data on reaction (1) at 10.1 GeV/c). For most of the data, the background is entirely negligible.

The data were normalized as follows. In the 10.1 GeV/c 1-arm experiment, the use of (for example) π^- beam tracks through the forward spectrometer when taking the $K^-p \to \pi^-\Sigma^+$ data, allowed a precise calibration of the Cerenkov and scintillation counter efficiencies, track reconstruction efficiencies, and absorption losses. Thus we were able to achieve a normalization precision of 3.4% on the cross-sections. The correction factors for the 7.0 GeV/c 1-arm data were readily deduced from those applied to the 10.1 GeV/c 1-arm data. The 2-arm data were subject to a slightly less precise normalization procedure, since here we also had to determine the trigger efficiency and detection efficiency for the recoil particles, as well as losses due to random vetoes from the counters round the target. In order to make these corrections, we took data for some of the time with different elements of the trigger relaxed, and data on several calibration reactions along with (1) and (2) viz. $\pi^\pm p$ elastic scattering, K^-p elastic scattering, and $\bar{p}p$ elastic scattering. These data also enabled us to confirm that the calculated absorption losses in the Monte-Carlo acceptance program were correct for both the forward arm and the recoil arm (where these losses were large at small $|t|$). Also we had at both momenta a substantial overlap in the t range covered by the 1-arm and 2-arm triggers. Thus the normalizations could be compared. We found

in all cases agreement at the level of 10%. In view of the very high precision of normalization of the 1-arm data, we finally renormalized the 2-arm data to exactly match the 1-arm data in the overlap region. Thus we estimate a maximum normalization error of 5%, of which many factors are common to both reactions.

In the 2-arm data, we required the recoil track to lie within the limits of the $\Sigma^+ \to p\pi^0$ decay cone. This eliminated between 80% and 90% of the $\Sigma^+ \to n\pi^+$ decays. We then determined the relationship between experimental asymmetry and polarization using the acceptance Monte Carlo. We smeared the Monte Carlo events by an amount determined from the precision in coplanarity measured with the elastic scattering data. We then imposed the same cuts on the recoil direction for the Monte Carlo events as were used on the hypercharge exchange data.

In fig. 2, we show the differential cross-sections and polarizations. Fig. 3 shows the differential cross-sections in the low $|t|$ region, and fig. 4 shows the relative cross-section differences Δ, where

$$\Delta = \frac{d\sigma/dt'(K^-p \to \pi^-\Sigma^+) - d\sigma/dt'(\pi^+p \to K^+\Sigma^+)}{d\sigma/dt'(K^-p \to \pi^-\Sigma^+) + d\sigma/dt'(\pi^+p \to K^+\Sigma^+)}$$

The data (which extend in to 0^0, ie $t'=0$) are most naturally binned in t'. For this reason, Δ is evaluated for bins in t' rather than t; the differences, however, are very small.

The cross-sections and polarization values are listed in tables I and II. Exponential fits have been made to the small $|t|$ data: parameters are shown in table III.

Turning to the s dependence of the differential cross-sections, we have determined the values of $\alpha_{eff}(t)$ (using the parametrization $d\sigma/dt(s,t)=f(t)*s^{2\alpha eff-2}$). Comparing our 7.0 GeV/c data for reaction (1) with that of Pruss et al.[2b] at the same momentum, we find agreement at the 10% level over the entire t range. We have therefore used data from their experiments[2b,2f] at 4 and 5 GeV/c together with our own data at 7.0 and

10.1 GeV/c. For reaction (2), we have used the high statistics experiment of Massaro et al.[2j] at 4.2 GeV/c together with our 7.0 and 10.1 GeV/c data. These results are shown in fig. 5 and listed in table IV. The results obtained using our data alone are in both cases consistent with those from the fits including the other experiments, but with larger errors due to the limited s range.

The behaviour revealed by the data may be described in terms of three regions of t, which merge smoothly into one another.

a) $t > -0.5$ $(GeV/c)^2$

We find near-equality of the cross-sections at t=0 for the 10.1 GeV/c data. Going out to $t=-0.5$ $(GeV/c)^2$, the ratio of cross-sections increases slowly to about 2.0. At 7.0 GeV/c, however, the cross-section ratios are larger, the value of Δ being on average twice as large as for the 10.1 GeV/c data. For reaction (2), the values of α_{eff} are closer to the K^*-K^{**} trajectory than those for reaction (1). The polarization grows rapidly to large values for both reactions, and shows approximate mirror symmetry, as has already been observed at lower momenta.

These results indicate the presence of an exchange-degeneracy violating contribution which becomes relatively larger with $|t|$, but decreases significantly between 7.0 and 10.1 GeV/c. In the limit of t=0 at the higher momentum, exchange degeneracy predictions are well satisfied.

b) $-0.6 > t > -0.8$ $(GeV/c)^2$

The differential cross-sections at both momenta show a cross-over. The values of α_{eff} lie quite well on the K^*-K^{**} trajectory. The polarization values remain large and approximately mirror-symmetric. These results suggest that the non exchange-degenerate contribution may be vanishing in this t region.

c) $-1.0 > t > -2.0$ $(GeV/c)^2$

Beyond the cross-over point the differential cross-sections show significant flattening, compared with their original exponential form. The cross-sections for the two reactions do not converge significantly as the momentum goes from 7.0 to 10.1 GeV/c (see values of Δ in fig. 4). The results obtained when the lower energy experiments are included would imply that the cross-sections are even diverging from one another (since the values of α_{eff} for reaction (1) are larger than those for reaction (2)). The polarization values decrease slowly through the t range.

These results suggest the presence of relatively larger exchange-degeneracy violating contributions in this t region than at lower $|t|$.

In summary, we find only small discrepancies with the predictions of weak exchange degeneracy at 10.1 GeV/c in the small $|t|$ region. However, the predictions of strong exchange degeneracy are not satisfied. At the lower momentum of 7.0 GeV/c, the data are inconsistent with the predictions of both strong and weak exchange degeneracy. The data at large $|t|$ show the largest deviations from the exchange degeneracy predictions with no clear improvement by 10.1 GeV/c. Finally we conclude that our measurements of both the differential cross-sections and polarizations of reactions (1) and (2) made in the same apparatus and at different momenta should provide considerable constraints on the theory of hypercharge exchange reactions.

It is a pleasure to thank John Lindsay and Michael Burns of CERN for their valuable assistance with the large capacitive readout system (10^5 wires) used on the spark chambers.

References

1. A. Berglund, T. Buran, P.J. Carlson, C.J.S. Damerell, I. Endo, A.R. Gillman, V. Gracco, R.J. Homer, M.J. Hotchkiss, A. Lundby, M. Macri, B.N. Ratcliff, A. Santroni, T. Tso, F. Wickens, J.A. Wilson. Physics Letters 57B(1975)100

2. Measurements of $\pi^+p \to K^+\Sigma^+$

a) 3.5, 3.75, 4, 4.25, 5, 6, 10, 14 GeV/c
A. Bashian, G. Finocchiaro, M.L. Good, P.D. Grannis, O. Guisan, J. Kirz, Y.Y. Lee, R. Pittman, G.C. Fischer, D.D. Reeder. Phys. Rev. D4(1971)2667

b) 3, 3.25, 4.00, 5.05, 7 GeV/c
S.M. Pruss, C.W. Akerlof, D.I. Meyer, S.P. Ying, J. Lales, R.A. Lundy, D.R. Rust, C.E.W. Ward, D.D. Yovanovitch. Phys. Rev. Lett. 23(1969)189

c) 3, 5, 7 GeV/c
P. Kalbaci, C.W. Akerlof, P.K. Caldwell, C.T. Coffin, D.I. Meyer, P. Schmueser, K. C. Stanfield. Phys. Rev. Lett. 27(1971)74

d) 5.4 GeV/c
W.A. Cooper, W. Manner, B. Musgrave, L.V. Voyvodic. Phys. Rev. Lett. 20(1968)472

e) 5 GeV/c
C.W. Akerlof, P.K. Caldwell, P. Kalbaci, D.I. Meyer, K.C. Stanfield, P.N. Kirk, A. Lesnik, D.R. Rust, C.E. W. Ward, D.D. Yovanovitch. Phys. Rev. Lett. 27(1971)219

f) 3, 4, 5 GeV/c
K.S. Han, C.W. Akerlof, P. Schmueser, P.N. Kirk, D.R. Rust, C.E.W. Ward, D.D. Yovanovitch, S.M. Pruss. Phys. Rev. Lett. 24(1970)1353

Measurements of $K^-p \to \pi^-\Sigma^+$

g) 8, 16 GeV/c
D. Birnbaum, R.M. Edelstein, N.C. Hien, T.J. McMahon, J.F. Mucci, J.S. Russ, E.W. Anderson, E.J. Bleser, H.R. Blienden, G.B. Collins, D. Garelick, J. Menes, F. Turkot. Physics Letters 21B(1970)484

h) 14.3 GeV/c
R.J. Miller, K. Paler, J.J. Phelan, T.P. Shah, B. Chaurand, B. Drevillon, G. Labrosse, R. Lestienne, D. Linglin, R.A. Salmeron, R. Barloutaud, A. Borg, C. Louedec, F. Pierre, M. Spiro. Nuovo Cimineto Lettere 6(1973)491 and Nucl. Phys. B117(1976)1

i) 4.07, 5.47 GeV/c
J.S. Loos, U.E. Kruse, E.L. Goldwasser. Phys. Rev. 173(1968)1330

j) 4.2 GeV/c
G.G.G. Massaro, S. Barley, A.J. de Groot, J.C. Kluyver, A.G. Tenner, Ph. Gavillet, J.B. Gay, R.J. Hemingway, S.O. Holmgren, M.J. Losty, F. Marzano, E.W. Kittel, R.T. van der Walle, H.G. Tiecke, R.T. Lamb P. Grossman, J. Wells. Phys. Lett 66B(1977)385

k) 3.95 GeV/c
L. Moscoso, J.R. Hubbard, A. Leveque, J.P. de Brion, C. Louedec, D. Revel, J. Badier, E. Barrelet, A. Rouge, H. Videau, I. Videau. Nuclear Physics B36(1972)332

3. K.W. Lai, J. Louie. Nuclear Physics B19(1970)205.

Table I. Differential cross-sections
Errors listed are statistical.

Reaction (1) $\pi^+p \to K^+\Sigma^+$ at 7.0 GeV/c momentum

t' $(GeV/c)^2$	t $(GeV/c)^2$	bin width $(GeV/c)^2$	$d\sigma/dt$ $\mu b/(GeV/c)^2$	error $\mu b/(GeV/c)^2$
-0.055	-0.0650	0.01	160.0	28.2
-0.070	-0.0800	0.02	172.5	15.9
-0.090	-0.1000	0.02	119.0	10.3
-0.110	-0.1200	0.02	124.4	7.8
-0.140	-0.1500	0.04	93.4	5.0
-0.180	-0.1900	0.04	65.0	3.8
-0.220	-0.2300	0.04	42.2	2.9
-0.260	-0.2700	0.04	27.0	2.3
-0.310	-0.3200	0.06	21.1	1.7
-0.370	-0.3800	0.06	11.3	1.2
-0.500	-0.5100	0.20	6.21	0.50
-0.700	-0.7100	0.20	4.10	0.47
-0.900	-0.9100	0.20	3.80	0.46
-1.100	-1.1100	0.20	3.45	0.45
-1.300	-1.3100	0.20	2.06	0.36
-1.500	-1.5100	0.20	1.66	0.32
-1.700	-1.7100	0.20	0.71	0.22
-1.900	-1.9100	0.20	0.35	0.18

Reaction (2) $K^-p \to \pi^-\Sigma^+$ at 7.0 GeV/c momentum

t' $(GeV/c)^2$	t $(GeV/c)^2$	bin width $(GeV/c)^2$	$d\sigma/dt$ $\mu b/(GeV/c)^2$	error $\mu b/(GeV/c)^2$
-0.055	-0.0463	0.01	353.8	41.3
-0.070	-0.0613	0.02	284.6	16.0
-0.090	-0.0813	0.02	255.3	11.2
-0.110	-0.1013	0.02	235.7	11.1
-0.140	-0.1313	0.04	171.3	7.5
-0.180	-0.1713	0.04	132.4	6.4
-0.220	-0.2113	0.04	100.7	5.6
-0.260	-0.2513	0.04	78.6	5.0
-0.310	-0.3013	0.06	49.6	3.3
-0.370	-0.3613	0.06	33.9	2.8
-0.500	-0.4913	0.20	15.7	1.1
-0.700	-0.6913	0.20	6.78	1.24
-0.900	-0.8913	0.20	3.52	0.92
-1.100	-1.0913	0.20	3.14	0.88
-1.300	-1.2913	0.20	1.06	0.53
-1.500	-1.4913	0.20	0.87	0.51
-1.700	-1.6913	0.20	0.62	0.44

Reaction (1) $\pi^+ p \to K^+ \Sigma^+$ at 10.1 GeV/c momentum

t' $(GeV/c)^2$	t $(GeV/c)^2$	bin width $(GeV/c)^2$	$d\sigma/dt$ $\mu b/(GeV/c)^2$	error $\mu b/(GeV/c)^2$
-0.005	-0.0117	0.01	243.3	9.4
-0.015	-0.0217	0.01	230.8	8.2
-0.025	-0.0317	0.01	200.9	7.5
-0.035	-0.0417	0.01	183.2	7.3
-0.045	-0.0517	0.01	174.2	7.4
-0.055	-0.0617	0.01	142.2	7.2
-0.065	-0.0717	0.01	146.8	8.1
-0.080	-0.0867	0.02	118.0	5.7
-0.100	-0.1067	0.02	103.4	6.1
-0.130	-0.1367	0.04	78.1	4.8
-0.175	-0.1817	0.05	53.3	4.2
-0.225	-0.2317	0.05	29.4	1.7
-0.275	-0.2817	0.05	18.5	1.0
-0.325	-0.3317	0.05	12.6	0.9
-0.375	-0.3817	0.05	9.25	0.71
-0.425	-0.4317	0.05	5.87	0.55
-0.475	-0.4817	0.05	4.25	0.46
-0.550	-0.5567	0.10	3.64	0.31
-0.650	-0.6567	0.10	2.79	0.27
-0.750	-0.7567	0.10	2.43	0.25
-0.875	-0.8817	0.15	1.90	0.18
-1.025	-1.0317	0.15	1.45	0.16
-1.200	-1.2067	0.20	1.16	0.13
-1.400	-1.4067	0.20	0.85	0.11
-1.625	-1.6317	0.25	0.47	0.07
-1.875	-1.8817	0.25	0.22	0.05
-2.125	-2.1317	0.25	0.20	0.05
-2.500	-2.5067	0.50	0.04	0.02

Reaction (2) $K^- p \to \pi^- \Sigma^+$ at 10.1 GeV/c momentum

t' $(GeV/c)^2$	t $(GeV/c)^2$	bin width $(GeV/c)^2$	$d\sigma/dt$ $\mu b/(GeV/c)^2$	error $\mu b/(GeV/c)^2$
-0.005	0.0011	0.01	301.0	27.4
-0.015	-0.0089	0.01	278.7	19.6
-0.025	-0.0189	0.01	222.2	16.9
-0.035	-0.0289	0.01	222.9	17.2
-0.045	-0.0389	0.01	225.5	18.1
-0.055	-0.0489	0.01	194.7	18.0
-0.065	-0.0589	0.01	171.2	18.4
-0.080	-0.0739	0.02	170.0	14.8
-0.100	-0.0939	0.02	158.0	16.7
-0.130	-0.1239	0.04	111.7	12.4
-0.175	-0.1689	0.05	74.3	6.8
-0.225	-0.2189	0.05	43.4	4.8
-0.275	-0.2689	0.05	28.1	3.9
-0.350	-0.3439	0.10	18.9	2.6
-0.500	-0.4939	0.20	7.97	1.20
-0.750	-0.7439	0.30	2.16	0.50
-1.100	-1.0939	0.40	0.60	0.23
-1.650	-1.6439	0.70	0.28	0.13

Table II. Polarizations

Reaction (1) $\pi^+p \to K^+\Sigma^+$ at 7.0 GeV/c momentum

t $(GeV/c)^2$	bin width $(GeV/c)^2$	polarization	error
-0.060	0.04	-0.03	0.26
-0.110	0.06	-0.14	0.13
-0.170	0.06	0.11	0.15
-0.300	0.20	0.23	0.12
-0.500	0.20	0.54	0.23
-0.800	0.40	0.72	0.21
-1.200	0.40	0.49	0.25
-1.700	0.60	0.09	0.36

Reaction (2) $K^-p \to \pi^-\Sigma^+$ at 7.0 GeV/c momentum

t $(GeV/c)^2$	bin width $(GeV/c)^2$	polarization	error
-0.080	0.08	-0.37	0.21
-0.160	0.08	-0.12	0.23
-0.300	0.20	-0.22	0.19
-0.600	0.40	-0.47	0.27
-1.200	0.80	-0.51	0.41

Reaction (1) $\pi^+p \to K^+\Sigma^+$ at 10.1 GeV/c momentum

t $(GeV/c)^2$	bin width $(GeV/c)^2$	polarization	error
-0.185	0.03	0.16	0.29
-0.225	0.05	0.21	0.16
-0.275	0.05	0.39	0.17
-0.350	0.10	0.66	0.14
-0.500	0.20	1.12	0.14
-0.700	0.20	0.94	0.17
-0.950	0.30	0.61	0.19
-1.300	0.40	0.53	0.19
-1.750	0.50	0.16	0.31

Reaction (2) $K^-p \to \pi^-\Sigma^+$ at 10.1 GeV/c momentum

t $(GeV/c)^2$	bin width $(GeV/c)^2$	polarization	error
-0.125	0.05	-0.22	0.28
-0.200	0.10	0.03	0.22
-0.350	0.20	-0.39	0.24
-0.675	0.45	-1.04	0.33
-1.450	1.10	0.13	0.67

Table III. Parameters of exponential fit of $d\sigma/dt$

We fit the differential cross-section in the range $0 > t > -0.4$ $(GeV/c)^2$ to the form $d\sigma/dt = A\, e^{bt}$.

7.0 GeV/c	$\pi^+p \to K^+\Sigma^+$	A= 338.0 ± 8.1	$\mu b/(GeV/c)^2$
		b= 8.96 ± 0.12	$(GeV/c)^{-2}$
	$K^-p \to \pi^-\Sigma^+$	A= 462.1 ± 8.2	$\mu b/(GeV/c)^2$
		b= 7.30 ± 0.08	$(GeV/c)^{-2}$
10.1 GeV/c	$\pi^+p \to K^+\Sigma^+$	A= 273.1 ± 3.4	$\mu b/(GeV/c)^2$
		b= 9.39 ± 0.09	$(GeV/c)^{-2}$
	$K^-p \to \pi^-\Sigma^+$	A= 292.4 ± 7.4	$\mu b/(GeV/c)^2$
		b= 8.36 ± 0.08	$(GeV/c)^{-2}$

Table IV. Values of $\alpha_{eff}(t)$

These are based on the present experiment, and on data of Pruss et al.[2b] at 4 and 5 GeV/c, and on data of Han et al.[2f] at 4 and 5 GeV/c for reaction (1), and on the data of Massaro et al.[2j] at 4.2 GeV/c for reaction (2).

The t values chosen are close to the t values used for the present experiment. Cross-sections and their errors are in general interpolated to these values from the published data where these are at different values of t.

Reaction (1) $\pi^+p \to K^+\Sigma^+$

t $(GeV/c)^2$	α_{eff}	error
-0.10	0.61	0.04
-0.15	0.55	0.04
-0.20	0.52	0.04
-0.25	0.46	0.04
-0.30	0.43	0.04
-0.40	0.40	0.06
-0.50	0.12	0.07
-0.70	-0.10	0.06
-0.90	-0.39	0.07
-1.10	-0.62	0.07
-1.30	-0.59	0.08
-1.50	-0.71	0.09
-1.70	-0.80	0.12
-1.90	-0.80	0.16

Reaction (2) $K^-p \to \pi^-\Sigma^+$

t $(GeV/c)^2$	α_{eff}	error
-0.05	0.45	0.06
-0.10	0.50	0.05
-0.15	0.34	0.05
-0.20	0.29	0.06
-0.25	0.30	0.07
-0.30	0.22	0.08
-0.40	0.15	0.08
-0.70	-0.16	0.13
-0.90	-0.63	0.15
-1.10	-0.99	0.18
-1.30	-1.19	0.21
-1.60	-1.30	0.23

Figure Captions

Fig. 1 Experimental layout (for the 2-arm set-up). The incident beam hodoscopes (to define the direction and momentum) and beam Cerenkov counters are not shown. T1-T4 are scintillation counter hodoscopes. C1 is a pressurised Cerenkov counter, set to count pions in the negative reaction and pions and kaons in the positive reaction. C2 is an atmospheric pressure Cerenkov hodoscope, set to count pions. W1 - W10 are spark chamber modules, each with 4 planes of wires read out. Some typical trajectories in the forward arm are shown as well as a recoil track.

Fig. 2 Differential cross-sections and polarizations for the two reactions at 7.0 GeV/c (a) and 10.1 GeV/c (b). The errors plotted are statistical.

Fig. 3 Differential cross-sections over the low $|t|$ region at 7.0 GeV/c (a) and 10.1 GeV/c (b). The errors plotted are statistical. The straight lines represent exponential fits to the data.

Fig. 4 Relative cross-section differences Δ as a function of t', at 7.0 GeV/c and 10.1 GeV/c.

Fig. 5 α_{eff} as a function of t based on the differential cross-sections of the present experiment and others at lower momenta (see text).

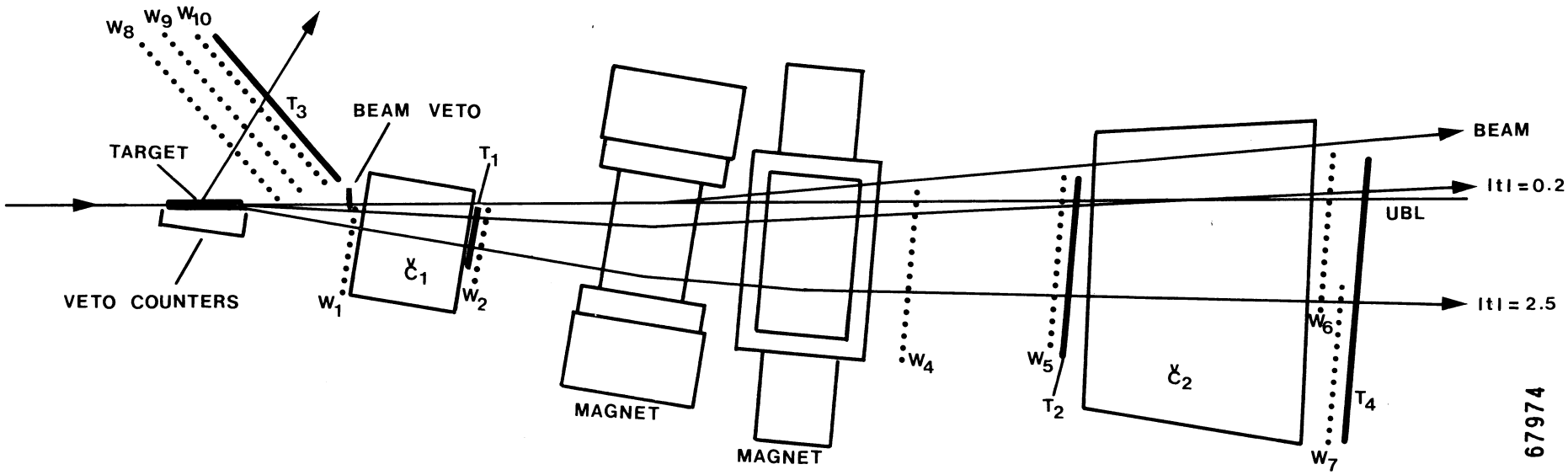
W8
W9
W10
T3
BEAM VETO
TARGET
T1
BEAM
|t| = 0.2
UBL
|t| = 2.5
VETO COUNTERS
W1
C1
W2
MAGNET
W4
W5
T2
C2
W6
T4
MAGNET
W7
67974

Fig 1

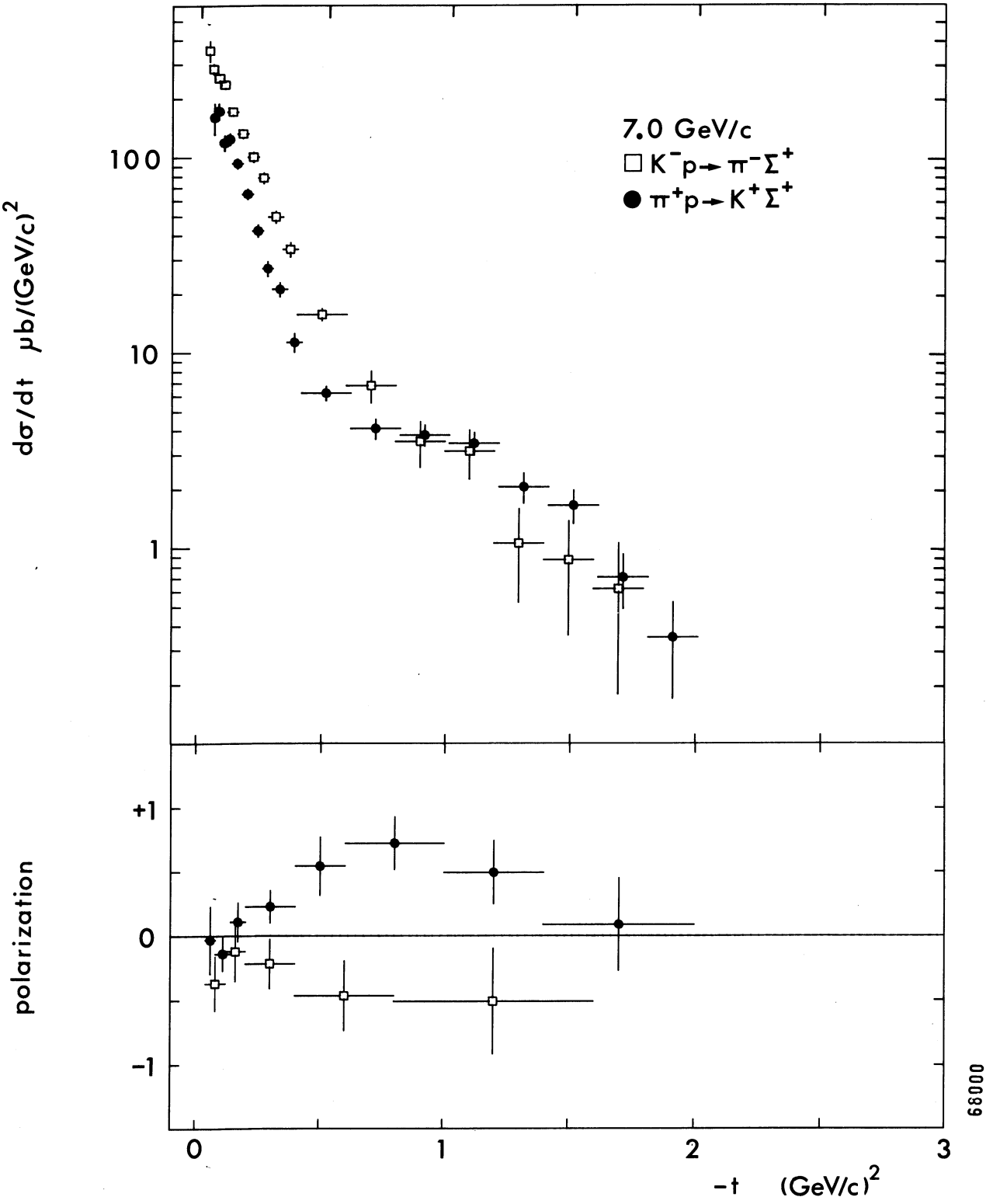
7.0 GeV/c
□ K⁻p→π⁻Σ⁺
● π⁺p→K⁺Σ⁺
dσ/dt μb/(GeV/c)²
100
10
1
polarization
+1
0
-1
0
1
2
3
-t (GeV/c)²
66000

Fig 2a

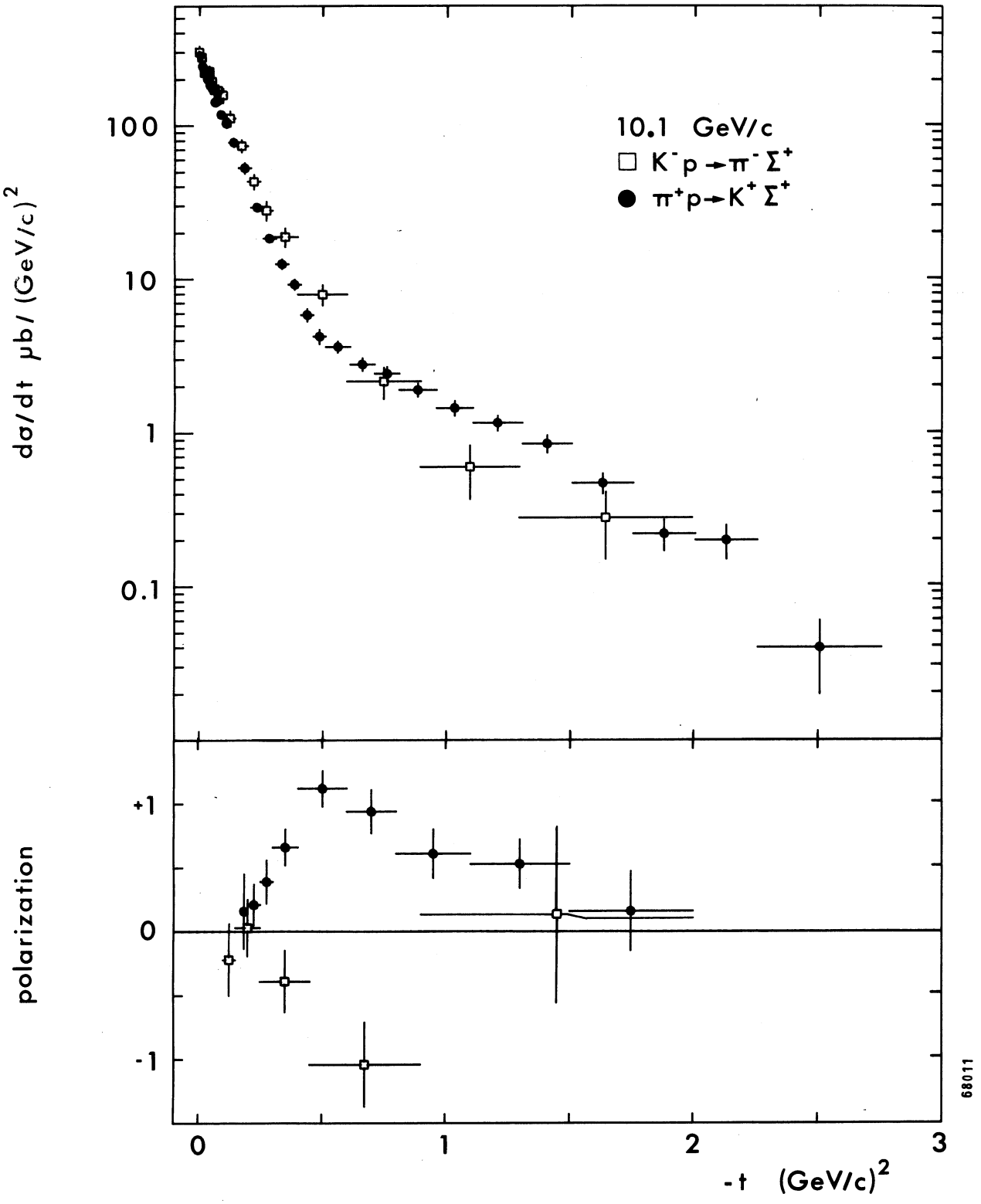
10.1 GeV/c
□ K⁻p → π⁻Σ⁺
● π⁺p → K⁺Σ⁺
dσ/dt μb/(GeV/c)²
100
10
1
0.1
polarization
+1
0
-1
0
1
2
3
-t (GeV/c)²
68011

Fig 2b

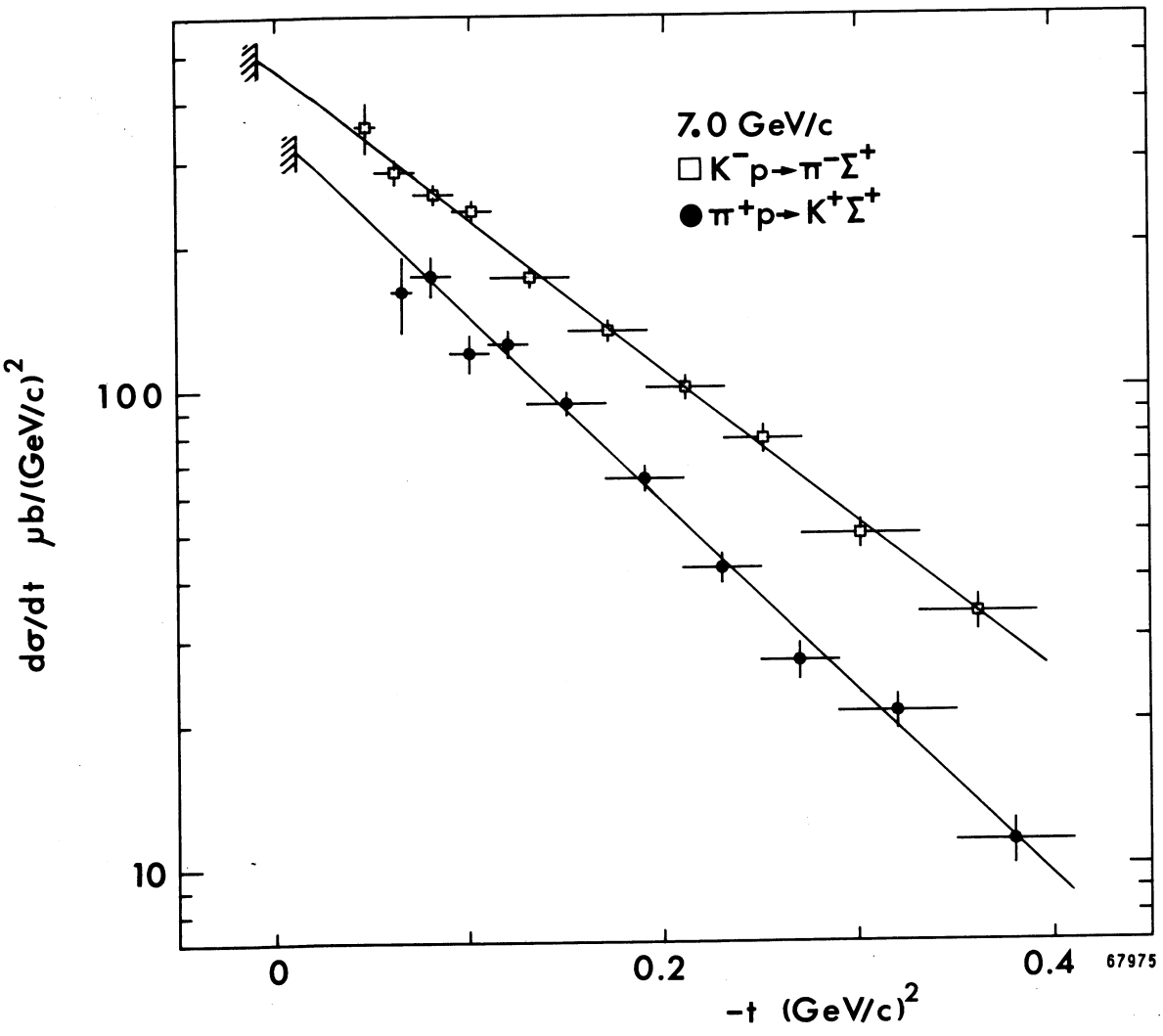

Fig 3a

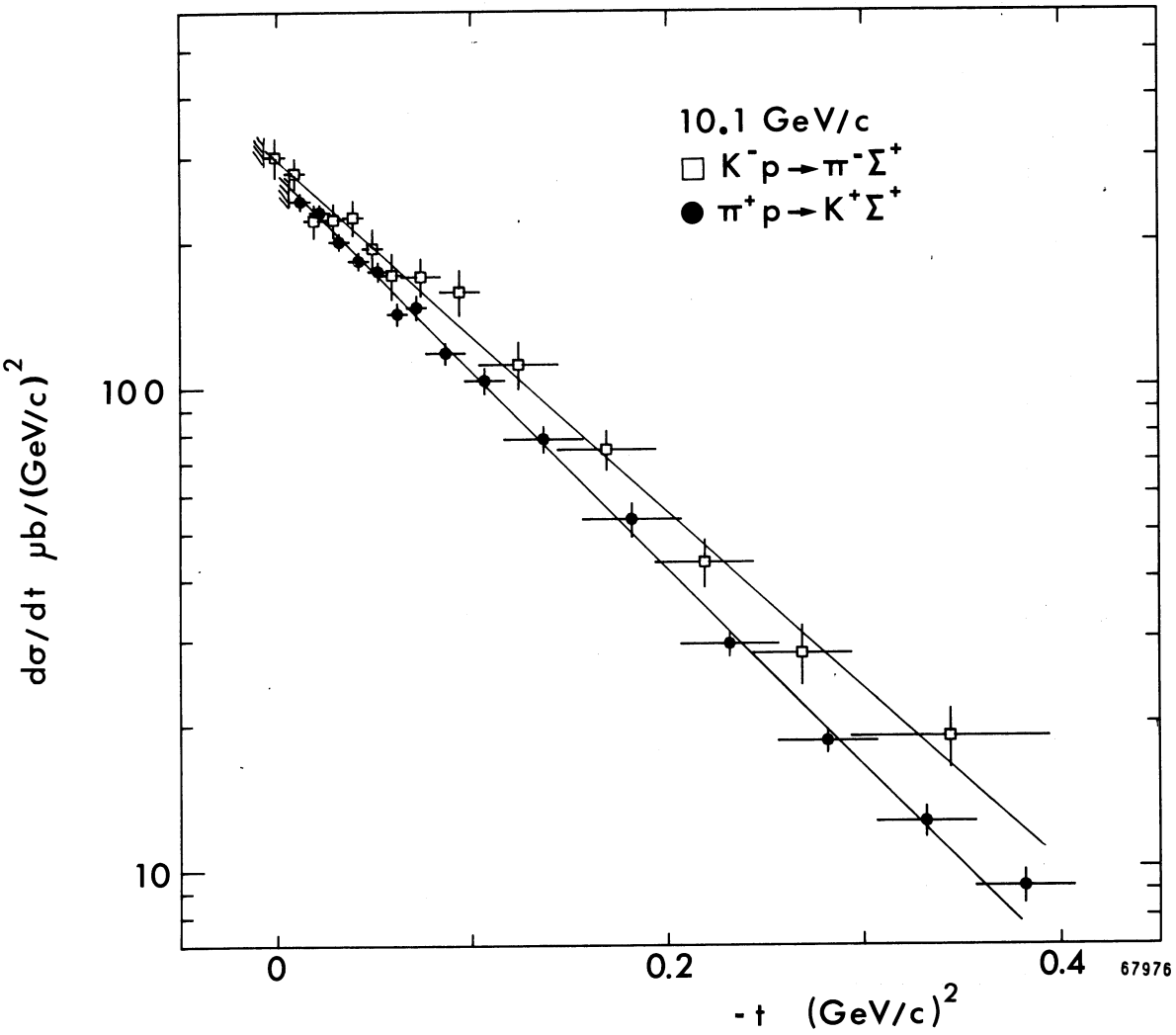

Fig 3b

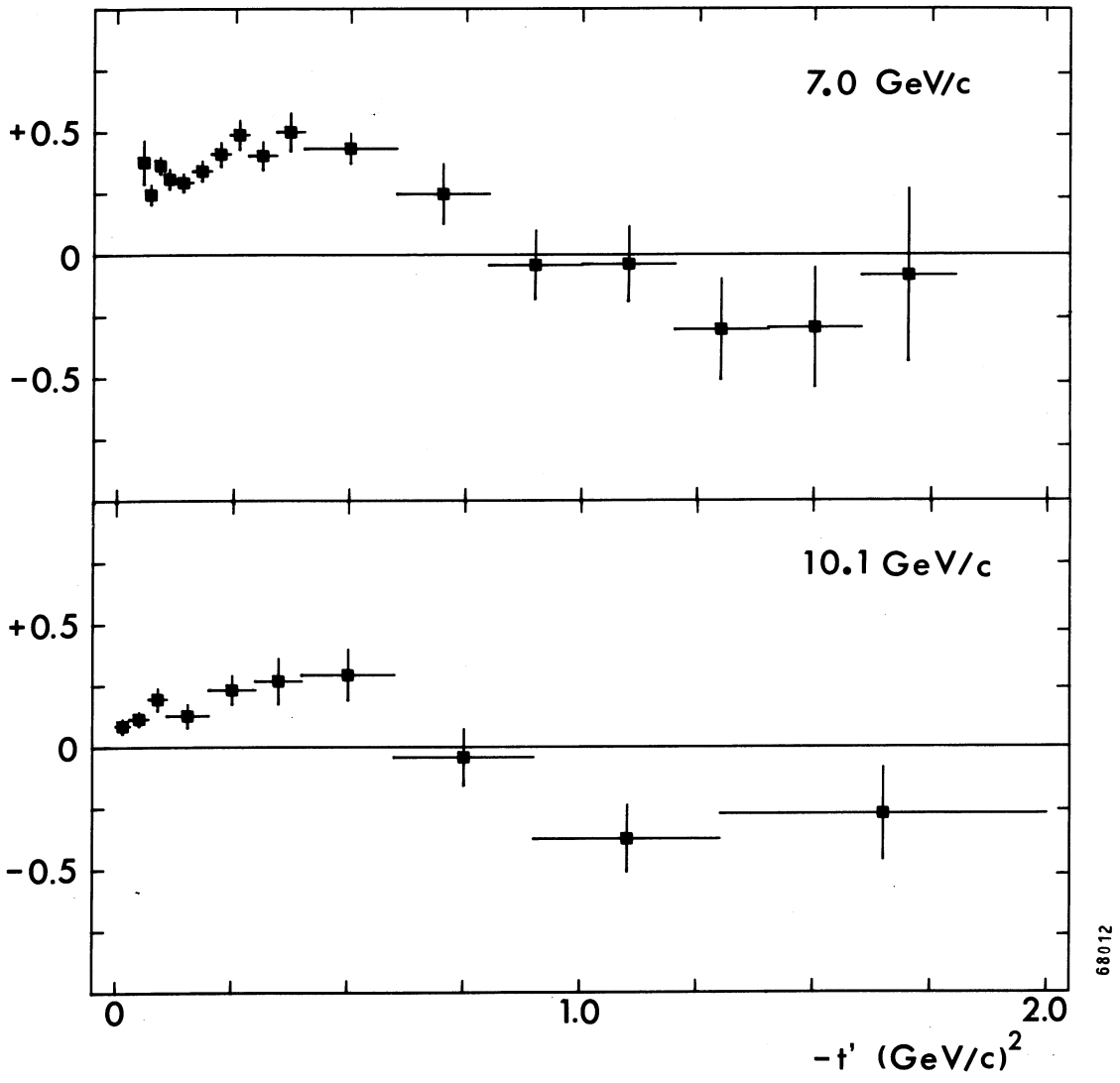

Fig 4

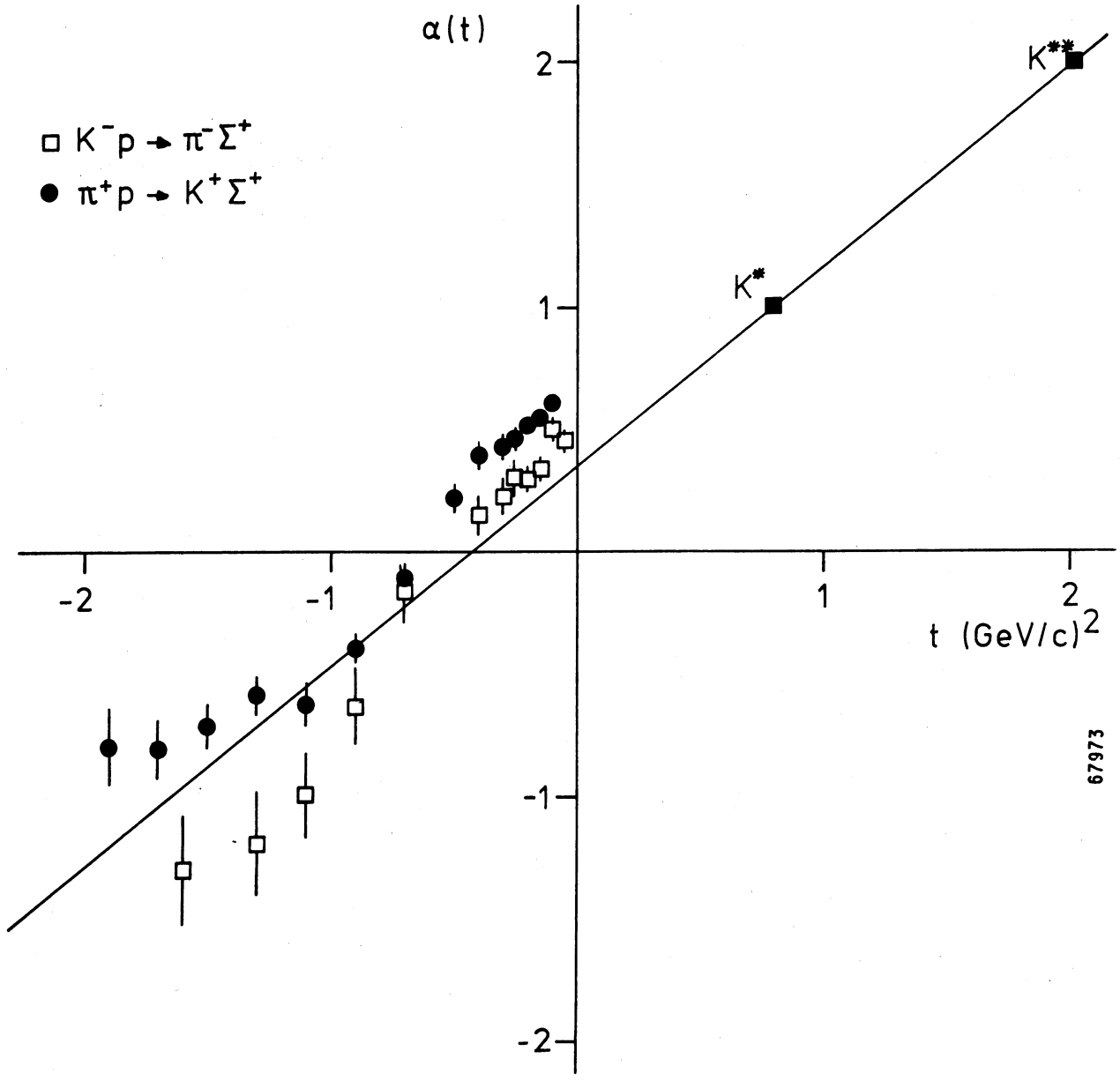

Fig 5